Reanalysis of the 1761 transatlantic tsunami

Martin Wronna[1,3], Maria Ana Baptista[1,2], Jorge Miguel Miranda[1,3]

1 Instituto Dom Luiz, Faculdade de Ciências da Universidade de Lisboa, Portugal
2 Instituto Superior de Engenharia de Lisboa, Instituto Politécnico de Lisboa, Portugal
3 Instituto Português do Mar e da Atmosfera, IP, Lisboa, Portugal

Correspondence to: Martin Wronna (Mawronna@fc.ul.pt)

Abstract. The segment of the Africa-Eurasia plate boundary between the Gloria fault and the Strait of Gibraltar has been the set of significant tsunamigenic earthquakes. However, their precise location and rupture mechanism remains poorly understood. The investigation of each event contributes to a better understanding of the structure of this diffuse plate boundary and ultimately leads to a better evaluation of the seismic and tsunami hazard. The 31st March 1761 event is one of the few known transatlantic tsunamis. Macroseismic data and tsunami travel times were used in previous studies to assess its source area. However, no one discussed the geological source of this event. In this study, we present a reappraisal of tsunami data to show that the observations dataset is compatible with a geological source close to Coral Patch and Ampere seamounts. We constrain the rupture mechanism with plate kinematics and the tectonic setting of the area. This study favors the hypothesis that the 1761 event occurred southwest of the likely location of the 1st November 1755.

1. Introduction

The coast along the southwest Iberian margin is prone to earthquakes and tsunamis. The earthquake and tsunami catalogs for the Iberian Peninsula and Morocco report three tsunamigenic earthquakes in the 18th century: 1722, 1755 and 1761 (Mezcua and Solares, 1983; Oliveira, 1986; Baptista and Miranda, 2009). While the 1722 event is believed to be a local event (Baptista et al., 2007), the 1st November 1755 and the 31st March 1761 earthquakes generated transatlantic tsunamis (Baptista et al., 1998a; Baptista et al., 2003; Baptista et al., 2006; Barkan et al., 2009). The source of the 1755 event has been extensively studied in recent years e.g. Baptista et al. (1998), Zitellini et al. (2001), Gutscher et al. (2006) and Barkan et al. (2009).

On the contrary, the tectonic source of 31st March 1761 remains poorly understood. The seismic catalogs present different earthquake locations: 10.00 W, 37.00 N (Mezcua and Solares, 1983) or 10.50 W, 36.00 N (Oliveira, 1986). Baptista et al. (2006), used macroseismic intensity data and tsunami travel time observations to locate the source circa 13.00 W, 34.50 N and estimated the magnitude in 8.5. The source location obtained by Baptista et al. (2006) places the 1761 event southwest of the South West Iberian Margin (SWIM) in the outer part of the Gulf of Cadiz (Fig. 1).

The SWIM is dominated by large NE-SW trending structures limiting the Horseshoe Abyssal Plain (HAP). The large NE-SW striking structures are the Coral Patch fault (CPF), the Gorringe Bank fault (GBF), the Horseshoe fault (HSF) and the Marques de Pombal fault (MPF) (Fig. 1). To the south, the HAP is limited by the igneous Ampere and Coral Patch seamounts. The present day tectonic regime is constrained by NW-SE plate convergence between Africa and Eurasia at ~4 mm/yr (Argus et al., 1989; DeMets et al., 1994) and westward migration of the Cadiz Subduction slab ~2 mm/yr (Gutscher et al., 2012; Duarte et al., 2013).

Figure 1. Source location by Baptista et al. (2006) and the tsunami observation points of the tsunami in 1761. The main features of the Azores Gibraltar fracture zone are the Azores Triple Junction (ATJ), the Gloria Fault (GF) and the Southwest Iberian Margin (SWIM). The inset shows the position of the Ampere seamount (Amp-SMT), the Coral Patch Seamount (CP-SMT) and the locations of the known faults. The black lines mark the faults, and the triangles indicate the direction of dip. The known faults are the Coral Patch Fault (CPF), the Cadiz Wedge Fault (CWF), the Gorringe Bank fault (GBF), the Horseshoe Fault (HSF) and the Marques de Pombal Fault (MPF).

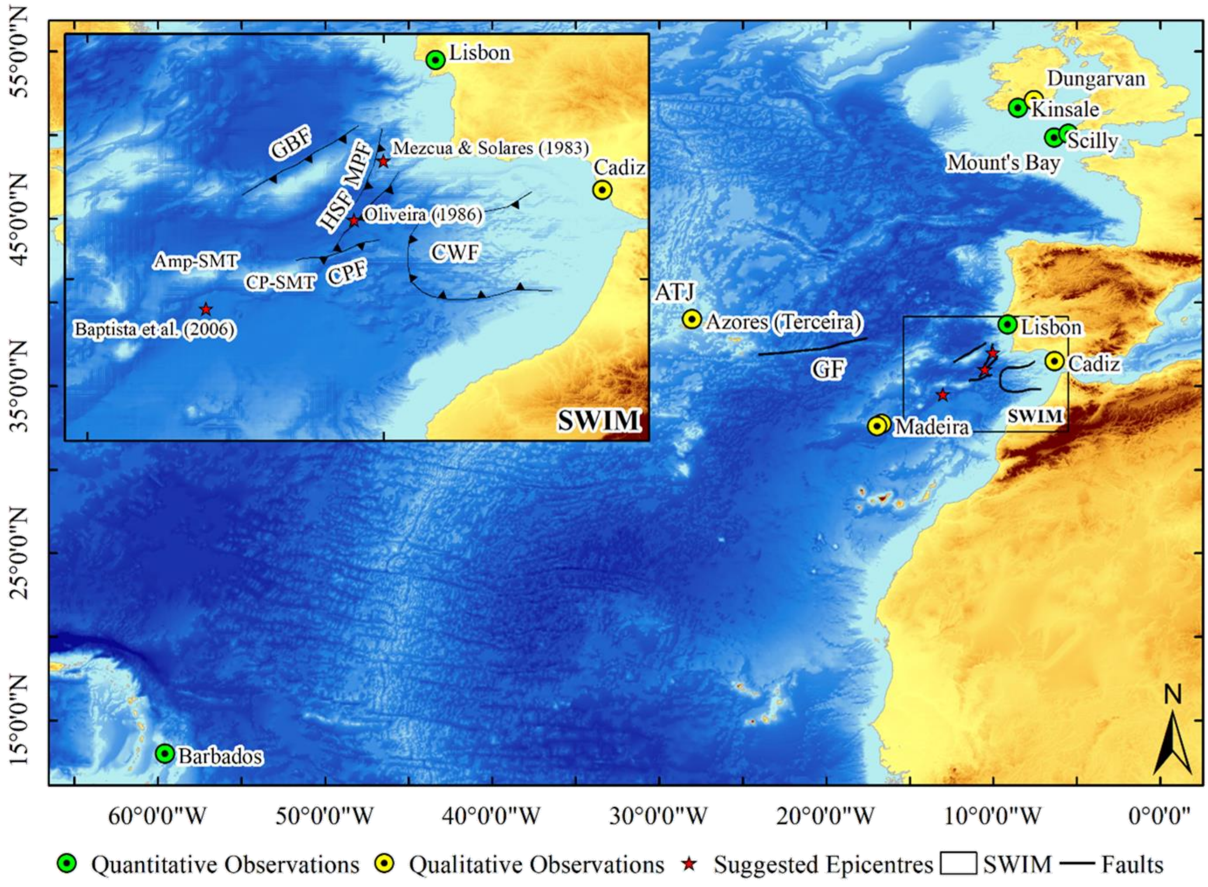

Figure 1. Source location by Baptista et al. (2006) and the tsunami observation points of the tsunami in 1761. The main features of the Azores Gibraltar fracture zone are the Azores Triple Junction (ATJ), the Gloria Fault (GF) and the Southwest Iberian Margin (SWIM). The inset shows the position of the Ampere seamount (Amp-SMT), the Coral Patch Seamount (CP-SMT) and the locations of the known faults. The black lines mark the faults, and the triangles indicate the direction of dip. The known faults are the Coral Patch Fault (CPF), the Cadiz Wedge Fault (CWF), the Gorringe Bank fault (GBF), the Horseshoe Fault (HSF) and the Marques de Pombal Fault (MPF).

In this study, we investigate the geological source of the 1761 transatlantic tsunami. To do this, we start with a reappraisal of previous research, we analyze the tectonic setting of the area and propose a source compatible with plate kinematics. From this source we compute the initial sea surface displacement. To propagate the tsunami, we build a bathymetric dataset based on GEBCO (2014) data to compute wave heights offshore the observations points presented in table 1. We also compute inundation using high resolution digital elevations models in Lisbon and Cadiz to compare the results with the observations. Finally, we use Cadiz and Lisbon observations in 1755 and 1761 to compare the size of the events.

2. Geodynamical context

The western segment of the plate boundary between Africa and Eurasia in the NE Atlantic Ocean extends from the Azores Triple Junction (ATJ) to Gibraltar. The main features of the Azores Gibraltar fracture zone are the ATJ; the Gloria Fault (GF) and the SWIM (Fig. 1). At the ATJ, the plate boundary is defined by active interplate deformation (Fernandes et al., 2006). The GF is a large W-E striking transverse fault with scarce seismicity (Laughton and Whitmarsh, 1974) with a strong magnitude event on 25th November 1941 (Gutenberg and Richter, 1949; Moreira, 1984; Baptista et al., 2016). The Gloria fault defines a sharp boundary between Eurasia and Africa (Laughton and Whitmarsh, 1974). Further East, towards the Gulf of Cadiz, in the SWIM area the plate boundary is not clearly defined (Zitellini et al., 2009). Large scale dynamics are imposed by convergence between Africa and Eurasia and by the westward propagation of the Gibraltar arc. Most recent studies agree that the source of the 1755 Lisbon earthquake with a magnitude of about 8.5±0.3 is in the SWIM (Johnston, 1996; Baptista et al., 1998; Zitellini et al., 1999; Gutscher et al., 2002; Solares and Arroyo, 2004; Ribeiro et al., 2006). Identified faults in the SWIM include large NE-SW trending thrust faults namely the Horseshoe Fault (HSF), the Marquês de Pombal fault (MPF), the Gorringe bank fault (GBF) and the Coral Patch fault (CPF) (Fig. 1). The GBF and the CPF bound the Horseshoe Abyssal Plain (HAP) and the aseismic SWIM-Lineaments – WNW-ESE trending dextral strike-slip faults (Zitellini et al., 2009). The NE-SW striking thrusts are deep rooted faults accompanied with morphological seafloor signatures. Moderate and small magnitude events (M<5) characterize the seismicity of the area. These faults lie between the Gorringe Bank and the Strait of Gibraltar (Custódio et al., 2015). South of the HAP the Coral Patch ridge shows surface deformation, with a predominating flower structure geometry (Rosas et al., 2009; Terrinha et al., 2009; Martínez-Loriente et al., 2013).

Considering the earlier mentioned faults, the CPF is closest to the area suggest by Baptista et al. (2006). Also, this area southwest of the SWIM, is in a slow deforming compressive regime dictated by the major tectonic driving forces (Eurasia – Africa convergence and Gibraltar arc westward propagation). The IGN seismic catalogs list a 6.2 magnitude around the Coral Patch on 11th of July 1915.

Kinematic plate models (Argus et al., 1989; DeMets et al. 1999; Nocquet and Calais 2004; Fernandes et al., 2007) predict low convergence rates 3 - 5 mm per year between African plates and Eurasia. We used the global kinematic plate model Nuvel-1A. This model is a recalibrated version of the precursor model Nuvel-1 that implements rigid plates and data from plate boundaries such as spreading rates, transform fault azimuths, and earthquake slip vectors (DeMets et al., 1990). The NUVEL

1A model predicts a relatively conservative convergence rate of 3.8 mm per year in the area close to the source area determined by Baptista et al. (2006) for the 1761 tsunami (Fig. 2).

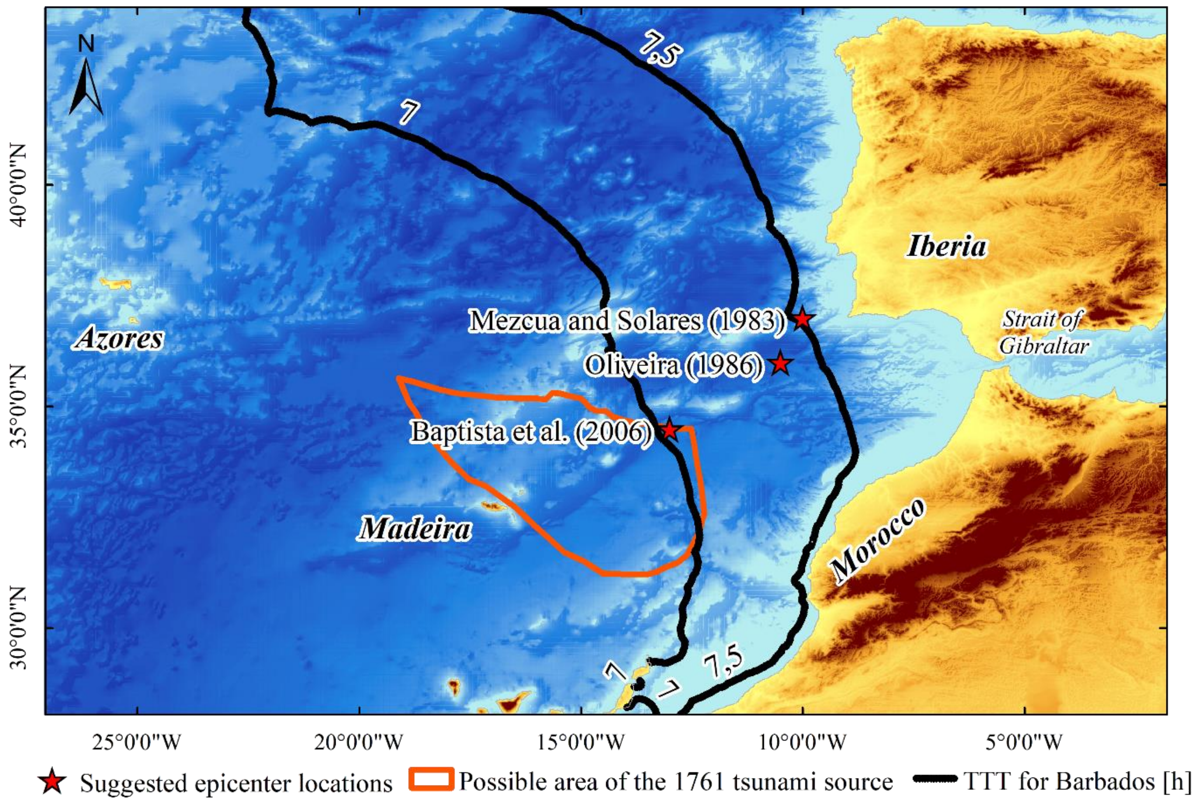

Figure 2. Source locations and backward ray tracing contours (black lines) for TTT of 7 – 7.5 hours to Barbados. The orange limited area defines the results obtained using macroseismic analysis combined with backward ray tracing but discarding the TTT for Barbados by Baptista et al. (2006).

Consequently, we consider a possible fault as an extension of the CPF closest to the area presented by Baptista et al. (2006). We draw the circle around the Euler pole at -20.61 w, 21.03 N according to the plate kinematic model Nuvel 1-A using Mirone suite (Luis 2007). To do this, we chose Africa as fixed plate and Eurasia as moving plate and draw the circle at the center of the fault in figure 3. We compute the convergence rate (3.8 mm per year) and plot the tangent velocity vector along the circle (Fig. 3). For this fault, we test different earthquake fault parameters and compute the co-seismic deformation using the Mansinha and Smiley equations (Mansinha and Smiley, 1971). We assume that the initial sea surface elevation mimics the sea bottom deformation and we use it to initiate the tsunami propagation model.

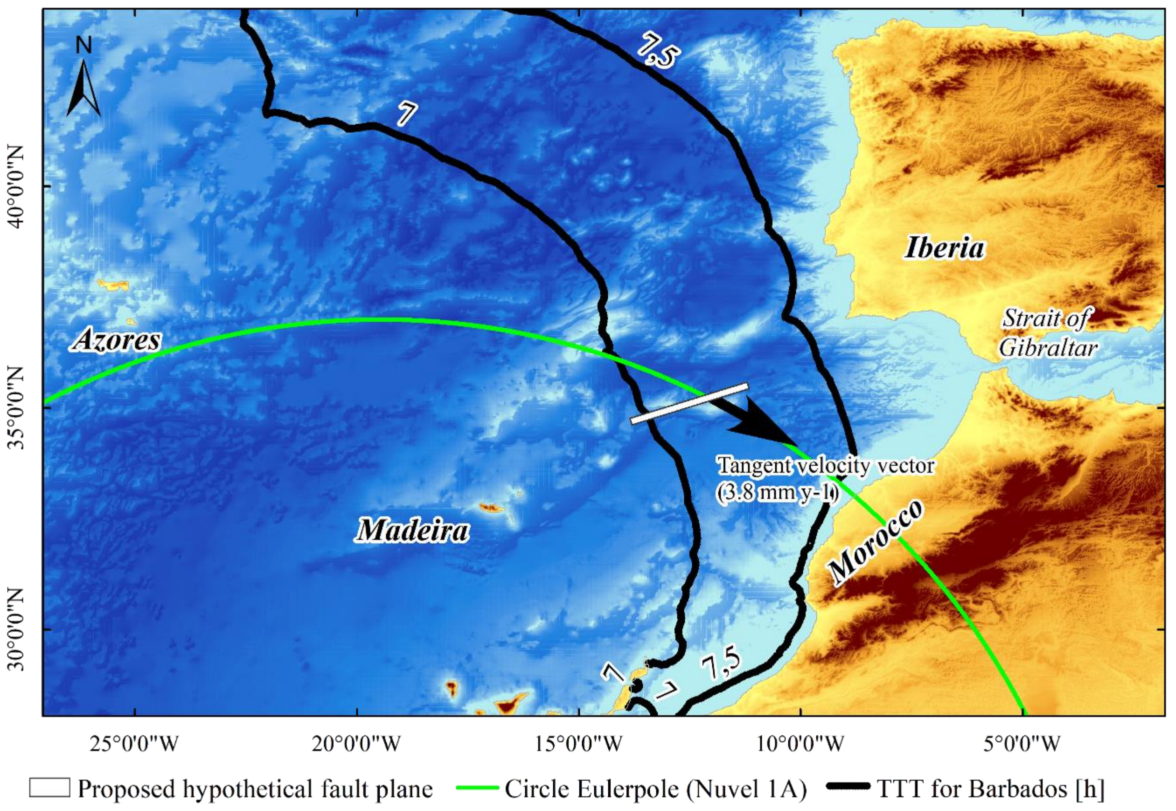

Figure 3. Circle around the Euler pole at the proposed hypothetical fault location. The model Nuvel 1A (DeMets et al., 1994, 1999) computes a 3.8 mm y^{-1} convergence. We plot the tangent velocity vector at the proposed fault. The black lines depict the backward ray tracing contours in hours, for TTT of 7-7.5 hours to Barbados.

3. Reassessment of historical data on the 1761 tsunami

The studies by Baptista et al. (2006) and Baptista and Miranda (2009) present most of the tsunami information used herein. However, only the information on tsunami travel times was used by these authors to locate the source (Baptista et al., 2006). In this study, we reappraise the tsunami observations regarding tsunami travel time and wave heights, period and duration of the sea disturbance.

For Cadiz, the Journal des Matiéres du Temps (Journal Historique, 1773), describes the occurrence of an earthquake in April 1773 and compares it with the 31st March 1761 event. The document states that in April 1773, following an earthquake felt in Cadiz, it was feared that it could have triggered a tsunami. The governor of the city ordered the closing of the town gates to prevent people fleeing to the causeway which was inundated in 1755. The report concludes that no tsunami was observed in 1773. However, the text of the report suggests a withdraw of the sea after the 31st March 1761 earthquake in the city.

We assume as in Baptista et al. (1998a, b) that all times are solar time and we re-evaluate the Tsunami Travel Time (TTT) for Barbados. Here, documents report a tsunami arrival at a 4 pm local time. Baptista et al. (2006) concluded for the unreliability of this observation and did not use it in the backward ray tracing simulations to locate the source. In this study, we use 3.5 hours solar time difference between Lisbon and Barbados. Using 4 pm local time as stated in Borlase (1762) for the arrival of the tsunami and the 3.5 h solar time difference between Lisbon and Barbados, we conclude that the TTT shoub be between 7-7.5 h. We place a point source at Barbados and use backward ray tracing and find that the 7 h contour falls within the area presented by Baptista et al. (2006) close to their suggested location (Fig. 1 and 2) at 34.50 N 13.00 W. Mason (1761) wrote that the tide ebbed and flowed between eighteen inches and two feet in Barbados.

The reports contain many observations about the abnormal motion of the sea. For Lisbon, the reports state abnormal motion of the sea about 1 hour and 15 minutes after the earthquakes. Two sources (Unknown, 1761 and Molloy, 1761) describe a flowing and ebbing of 8 feet of about six minutes while Borlase (1762) reports only three to four feet. All three reports agree that the agitation lasted until the evening.

The descriptions from northern Europe include Mount’s Bay, Scilly Islands, Kinsale and Dungarvan (Table 1 and Figure 1).

Borlase (1762) reports the tsunami observations at several points in Mount’s Bay. The waves arrived around five o’clock in the afternoon at about one and a half hour before full ebb. According to the report, the water rose between four and six feet, and the sea advanced and recessed five times within an hour (Table 1).

At Scilly Islands, the report states that the sea rose four feet and that the agitation lasted about 2 hours. In Kinsale, the Annual Register (1761) states that at 6 p.m. at low water, the tide rose quickly about two feet higher than it was and it ebbed again about four minutes later. The movement of the fluxes repeated several times but with decreasing intensity after the in and out flux. In Dungarvan, Borlase (1762) states that the sea ebbed and flowed five times between 4 and 9 o’clock in the afternoon.

Table 1 presents a summary of all historical data relevant to the tsunami simulation. Figure 1 shows the locations of the tsunami observations. Wave heights always refer to the maximum positive amplitude above the still water level.

Table 1. Summary of the available data of the 1761 tsunami at the time.

Location	Lon. [°]	Lat. [°]	Local Time	TTT [h]	Wave height [m]	Polarity	Period [min]	Duration	Source
Lisbon	-9.13	38.72°	13:15	1.25	1.2 - 1.8	-	6	Lasted until night	Unknown (1761); Molloy (1761); Borlase (1762)
Cadiz	-6.29	36.52	-	-	-	D	-	-	Journal des Matieres du Temps (1773)
Kinsale	-8.51	51.67	18:00	6	0.6	U	4	Repeated several times	Annual Register (1761); Borlase (1762)
Scilly Islands	-6.38	49.92	17:00	5	0.6 - 1.2	U	-	> 2 hours	Borlase (1762)
Mount's Bay	-5.48	50.08	17:00	5	1.2 - 1.8	U	12	1 hour	Borlase (1762)
Dungarvan	-7.48	51.95	16:00	4	-	-	-	5 hours	Borlase (1762)
Barbados	-59.57	13.03	16:00	7 - 8	0.45 - 0.6	-	8	4 hours but lasted until 6 in the morning.	Mason (1761); Annual Register (1761)
	-59.57	13.03			0.6	-	3 - 6	Increased again at ten for short time then decreased.	Borlase (1762)
Madeira	-16.91	32.62	-	-	~1; higher in the East	-	-	Lasted longer in the East than in the South.	Heberden (1761)
Azores	-27.22	38.65	-	-	Large	U	Some min.	3 hours	Fearns (1761)

4. Tsunami Simulations

4.1 The numerical model

We used the code NSWING (Non-linear Shallow Water model wIth Nested Grids) for numerical tsunami modeling. The code solves linear and non-linear shallow water equations (SWEs) in a Cartesian or spherical reference frame using a system of nested grids and a moving boundary condition to track the shoreline motion based on COMCOT (Cornell Multi-grid Coupled Tsunami Model; Liu et al., 1995; 1998). The code was benchmarked with the analytical tests presented by Synolakis et al. (2008) and tested in Miranda et al. (2014) and Baptista et al. (2016), Wronna et al. (2015) and Omira et al. (2015).

For Cadiz and Lisbon only, where high-resolution bathymetric data was available, we employed a set of coupled nested grids with a final resolution of 25 m to compute inundation. We compute a new bathymetric dataset using the nautical charts close to the coast or LIDAR data to build a Digital Terrain Model to compute inundation in Lisbon and Cadiz. Close to the tsunami source we interpolate bathymetry data (GEBCO, 2014) to obtain a 1600 m grid cell size. We apply a refinement factor of 4 for the four nested grids. Consequently, the intermediate grids have a resolution of 100 m and 400 m respectively. In Cadiz, we use the soundings and coastline of historical nautical charts from the 18th century (Bellin, 1762 and Rocque, 1762) to compute a Paleo Digital Elevation Model (PDEM) (Wronna et al., 2017). To do this, we geo-referenced the old nautical charts and use the modern-day DEM (UG-ICN, 2009) to implement the information from the ancient charts. According to Wronna et al. (2017) we systematically remodeled bathymetry and the coastline.

To initiate the tsunami propagation model, we compute the co-seismic deformation according to the half-space elastic theory (Mansinha and Smylie, 1971) implemented in Mirone suite (Luis, 2007). Assuming that water is an incompressible fluid we translate the sea bottom deformation to the initial sea surface deformation and set the velocity field to zero for the time instant t = 0 s. We run the model for 10-hour propagation time to ensure that the tsunami reaches all observation points.

We compute the offshore wave heights for points located close to the observation points (Fig. 1) using Virtual Tide Gauges (VTG). We include the coordinates and depths of the VTG in the tables 3 and 4 in section 5. For transatlantic propagation, we consider the Coriolis effect in the tsunami simulation. All tsunami simulations were checked against historical data.

For the locations in Ireland, the United Kingdom, the Azores, Madeira and Barbados we use the approximation according to the Greens Law (Green, 1838). The Greens Law is based on the linear shallow water wave equations and allows to quickly approximate the amplification of wave heights at a shallower depth close to the shore when considering a plane beach. The wave height increases to the fourth root of the ratio between the depth at the shore and the water depth at the VTG. We extrapolate the maximum wave height values between the depths of the VTG (table 3 and 4) to points located at 5 m depth.

$$h_s = \sqrt[4]{\frac{d_s}{d_d}} * h_d \qquad \text{Eq. (1)}$$

Where h_s and h_d are the wave heights at the shore and the VTG respectively, and d_s and d_d are the depths at the shore and the VTG respectively. For d_s we use a constant value of 5 m. the results of the approximation according to the Greens Law are presented in table 3 and 4.

4.2 Testing the hypothesis

In the 20th century, two strong magnitude earthquakes occurred in the Gloria Fault (GF) area. In view of this, we tested the compatibility of the tsunami observations in 1761 with the tsunamis produced by the earthquakes of the 25th November 1941 (Lynnes and Ruff, 1985; Baptista et al., 2016) and 26th May 1975 (Kaabouben et al., 2009). We use the fault plane parameters and rupture mechanism presented in Baptista et al. (2016) and Kaabouben et al. (2008) for the 1941 and 1975 events respectively. The fault dimensions and slip were made compatible with an 8.5 magnitude event using the scaling laws proposed by Wells and Coppersmith (1994), Manighetti et al. (2007) and Blaser et al. (2010).

These two events produce less than one-meter wave height in the North East Atlantic and were barely observed wave in the Caribbean Islands (Baptista et al., 2016; 2017). Moreover, the epicenters of the 25th November 1941 and 26th May 1975 are located outside the area determined by Baptista et al. (2006). As expected, the TTTs do not agree with those reported in 1761, therefore we excluded the GF as a candidate source for the 1761 event and do not consider their results for discussion.

The candidate fault area is centered at 12.00 W, 35.00 N to the west of the large NE/SW striking compressive structures (Martinez-Loriente et al., 2013) and 85 km northeast of the epicenter suggested by Baptista et al. (2006) (Fig. 3). We considered the fact that the historical accounts indicate an earthquake and tsunami less violent than the 1755. To account for this, we used the fault dimensions presented in table 2 corresponding to a magnitude 8.4-8.5 earthquake (Baptista et al., 2006), consequently the wave heights in Lisbon and Cadiz are smaller than those observed in the 1755 tsunami (Baptista et al., 1998). The fault dimensions presented in table 2 are compatible with the scaling laws of Wells and Coppersmith (1994), Manighetti et al. (2007) and Blaser et al. (2010).

Hypotheses A and A-MS: Here we use a strike angle compatible with the study by Martinez-Loriente et al., (2013) that follows the morphology of the Coral Patch seamount (Fig. 1). The velocity vector predicted by NUVEL 1A (Fig. 3) together with the short periods (4-12 minutes) reported in 1761 (table 1) are in line with the mean dip angle of 40 degrees suggested by Martinez-Loriente et al. (2013) (table 2). We approximate the rake angle according to the difference between the convergence arrow given by the circle around the Euler Pole and the fault plane (Fig. 3).

The wave period in Lisbon produced by this candidate source is 30 minutes. This value it is not compatible with the observations (Table 1). To solve this problem, we implemented a multi segment fault here called A-MS. This multi-segment solution consists of 4 segments each 50 km. The 4 segments are placed adjacent to each other and the rupture mechanism is equal for each segment as in hypothesis A with a mean slip of 11m (Table 2). The slip of each segment is presented in table 2. The synthetic waveforms are presented in figure 5 and discussed in sections 5 and 6.

Hypothesis B: Finally, we test an alternative hypothesis here called B with a larger strike-slip component compared to hypothesis A. This also results in larger fault length and a steeper dip angle. Here, we consider a rupture along a fault plane rotated about 180° when compared to hypothesis A. To do this, we selected compatible strike and rake angles that results in a sinistral inverse lateral rupture (table 2).

The synthetic waveforms are presented in figure 7 and discussed in sections 5 and 6.

Table 2. The fault dimensions and parameters used herein to investigate candidate sources of 1761 event. We describe hypotheses (Hyp.) A-MS, A and B by the fault parameters length (L), width (W), strike, dip, rake, slip and depth. The slip values for hypothesis A-MS are listed for each segment from west to east. Additionally, we present the moment magnitude (Mag.), the assumed shear modulus (μ) and the focal mechanism.

Scenario	L [km]	W [km]	Strike [°]	Dip [°]	Rake [°]	Slip [m]	Depth [km]	Mag.	μ [Pa]	Focal mechanism
Hyp. A-MS	4 x 50	50	76	40	135	7/15/15/8	10	8.4	$4*10^{10}$	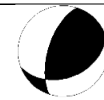
Hyp. A	200	50	76	40	135	11	10	8.4	$4*10^{10}$	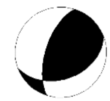
Hyp. B	280	50	254.5	70	45	15	10	8.5	$4*10^{10}$	

5. Results

We present the results of hypothesis A-MS and B. Hypothesis A-MS has a more significant inverse component compared to hypothesis B. Once the results of hypotheses A and A-MS produce equal wave height values, but the latter produces shorter periods, so we opt to present the results for hypothesis A-MS. Figures 4-7 show the maximum wave height and the synthetic tsunami at the virtual tide gauges (VTG) computed offshore of each observation point of hypothesis A-MS and B. Tables 3 and 4 summarize these results. The wave height, as mentioned in section 3, represents the maximum positive amplitude above the still water level, which is set to be 0 in the tsunami simulation. The geographical coordinates and depths of the VTGs are given in tables 3 and 4. To compare the synthetic wave heights with the observations for the locations in Mount's Bay, Scilly Islands, Kinsale, Dungarvan, Azores, Madeira and Barbados we used the Green's Law (Green, 1838) to extrapolate the wave height values for the maximum wave between the depths of the VTG to points located at 5 m depth. For Lisbon and Cadiz, where high-resolution bathymetry is available we used two sets of nested grids and computed the tsunami inundation. Here the VTGs are located close to the shore, and the application of the Green's Law is not necessary.

5.1 Hypothesis A-MS

Figures 4 and 5 show the distribution of the maximum wave height and the respective synthetic tsunami records for hypothesis A-MS.

Analysis of figure 4 shows wave heights exceeding 4 m in the Gulf of Cadiz. At some points along the coast of Morocco maximum wave heights are about 5 m. In Great Britain, at the Scilly Islands and Mount´s Bay maximum wave heights vary between 1.7 and 1.9 m. Along the south coast of Ireland, in Kinsale and Dungarvan the tsunami simulation predicts a 1 m maximum wave height. At the eastern coast of Madeira Island, the wave heights reach 1 m whereas on the southern part of the island the wave heights are smaller. At the Azores close to Terceira Island wave heights are slightly higher than 2.5 m along the south coast of the island. The wave heights in the south of Barbados reach 0.5 m.

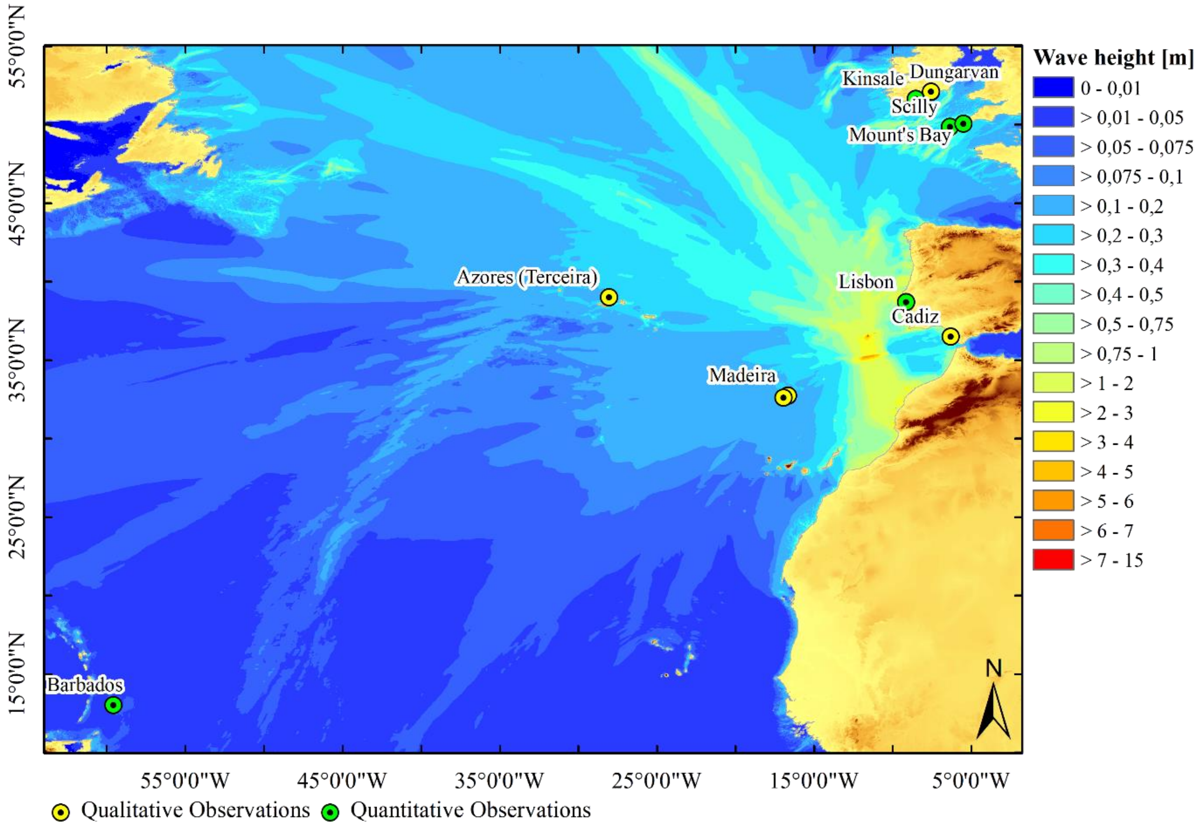

Figure 4. Maximum wave height distribution (color scale in m) in the Atlantic basin produced by the source of hypothesis A-MS.

In Lisbon, the synthetic waveform shows a first peak 1.4 m with a maximum value close to 1.8 m for the third wave, after two hours and twenty minutes of tsunami propagation. The TTT to Lisbon is 1 hour and 10 minutes and the first wave has a period of 20–25 minutes (table 3 and Fig. 5 (a)). In Cadiz, the synthetic tsunami waveform shows a drawdown 1 hour after the earthquake with a negative amplitude of 0.6 m and a maximum wave height of 2.4 m (table 3 and Fig. 5 (a)).
The Scilly Islands synthetic tsunami waveform shows a TTT of 4 hours and a maximum peak exceeding 0.4 m with a 15-minute period. In Mount´s Bay, TTT is 4 hours and 30 minutes and the maximum wave height is 0.5 m with 15 minutes period. In Kinsale, the tsunami model computes a TTT of 4 hours and 15 minutes. The maximum wave height there is about 0.5 m with a period shorter than 15 minutes. In Dungarvan, the tsunami arrives 5 hours after the earthquake. All VTGs in northern Europe recorded the first wave as leading elevation wave (Fig. 5 (b and c)).

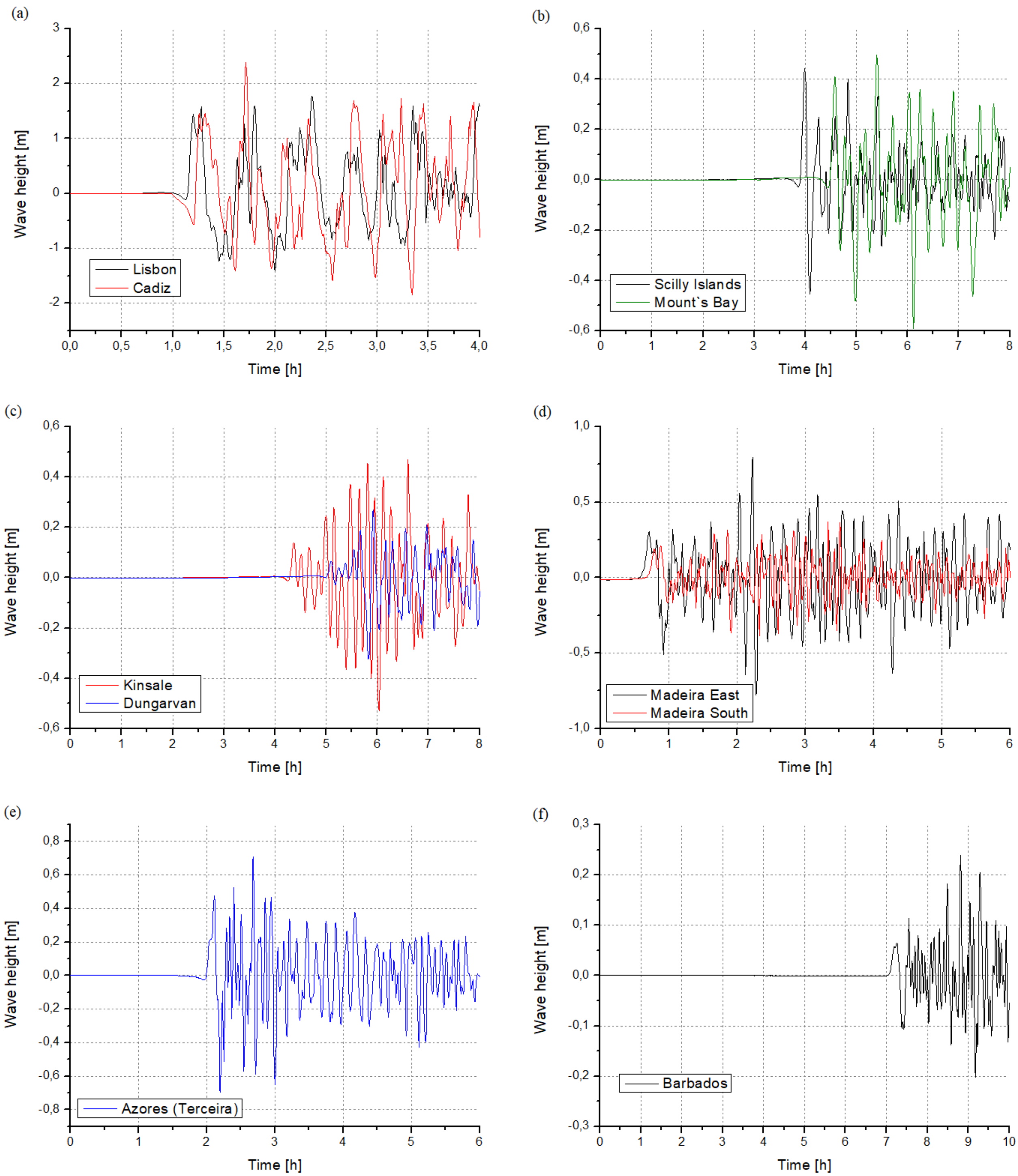

Figure 5. VTG records for hypothesis A-MS at the coordinates of the locations presented in table 3.

In Madeira, hypothesis A-MS produces maximum wave heights at the VTG of 0.8 m in the eastern part of the island and about 0.4 m, in the southern part; the TTT to the east and southern coast of the island is half an hour and 40 min respectively (Fig. 5 (d)). In the Azores, close to the island of Terceira, the wave heights reach approximately 0.7m (Fig. 5 (e)).

In Barbados, hypothesis A-MS produces the first wave of about 0.1 m after about 7 hours with about 30 minutes period. Only after 9 hours and 30 minutes, the wave height exceeds 0.2 m (Fig. 5(f)).

We applied the Green's Law in all locations except Lisbon and Cadiz to extrapolate the maximum wave height values to a depth of 5 m close to the shore to compare the values with the observations in section 3. The maximum wave height values after application of Green's Law are presented in table 3.

Table 3. Results of the VTGs for hypothesis A-MS

Local		**VTG coordinates & depth**			**TTT**	**Wave height [m]**				**Polarity**	**Period**
		Lon. [°]	Lat. [°]	d [m]		First	max.	Green's Law	Obs.		
Lisbon		-9.136	38.706	3	~ 1 h 10 min	1.6 m	1.8 m	nesting	1.2 – 1.8 m	D	< 30 min
Cadiz		-6.291	36.524	4	~ 1 h	-0.6 m	2.4 m	nesting	-	D	~ 30 min
Scilly Islands		-06.383	49.85	50	~ 4 h	0.4 m	0.4 m	0.7 m	0.6 – 1.2 m	U	~ 15 min
Mount´s Bay		-05.48	50.08	26	~ 4 h 30 min	0.4 m	0.5 m	0.8 m	1.2 – 1.8 m	U	~ 15 min
Kinsale		-08.500	51.653	28	~ 4 h 15 min	0.1 m	0.5 m	0.8 m	0.6 m	U	< 15 min
Dungarvan		-07.479	51.949	50	~ 5 h	0.1 m	0.3 m	0.5 m	-	U	< 15 min
Madeira	**E**	-16.666	32.750	51	~ 30 min	0.3 m	0.8 m	1.4 m	-	U	~ 30 min
	S	-16.926	32.619	51	~ 40 min	0.2 m	0.4 m	0.7 m	-	U	~ 30 min
Azores		-27.150	38.800	53	~ 2 h	0.5 m	0.7 m	1.3 m	-	U	~ 15 min
Barbados		-59.566	13.033	50	~ 7 h	0.1 m	0.2 m	0.4 m	0.45 – 0.6 m	U	~ 30 min

5.2 Hypothesis B

In Hypothesis B the dip angle was increased relative to hypothesis A resulting in the dominant strike-slip mechanism. In figure 6, we depict the maximum wave height for option B.

Analyzing figure 6 we find maximum wave heights of 15 m along the coast of Morocco. In the Gulf of Cadiz, the wave heights do not exceed 2 m. In Great Britain, at the Scilly Islands the maximum wave height is close to 2.3 m, and in Mount´s Bay, the maximum wave height values reach 1.8 m. For the locations in Ireland, Kinsale and Dungarvan, the maximum wave heights exceed 1.4 m. The eastern part of Madeira experiences wave heights greater than 2.5 m, decreasing towards the southern parts of the Island (Fig. 6). The maximum wave height exceeds 5.5 m on the eastern side of the island of Terceira in the Azores. For Barbados, this source computes maximum wave heights exceeding 0.7 m.

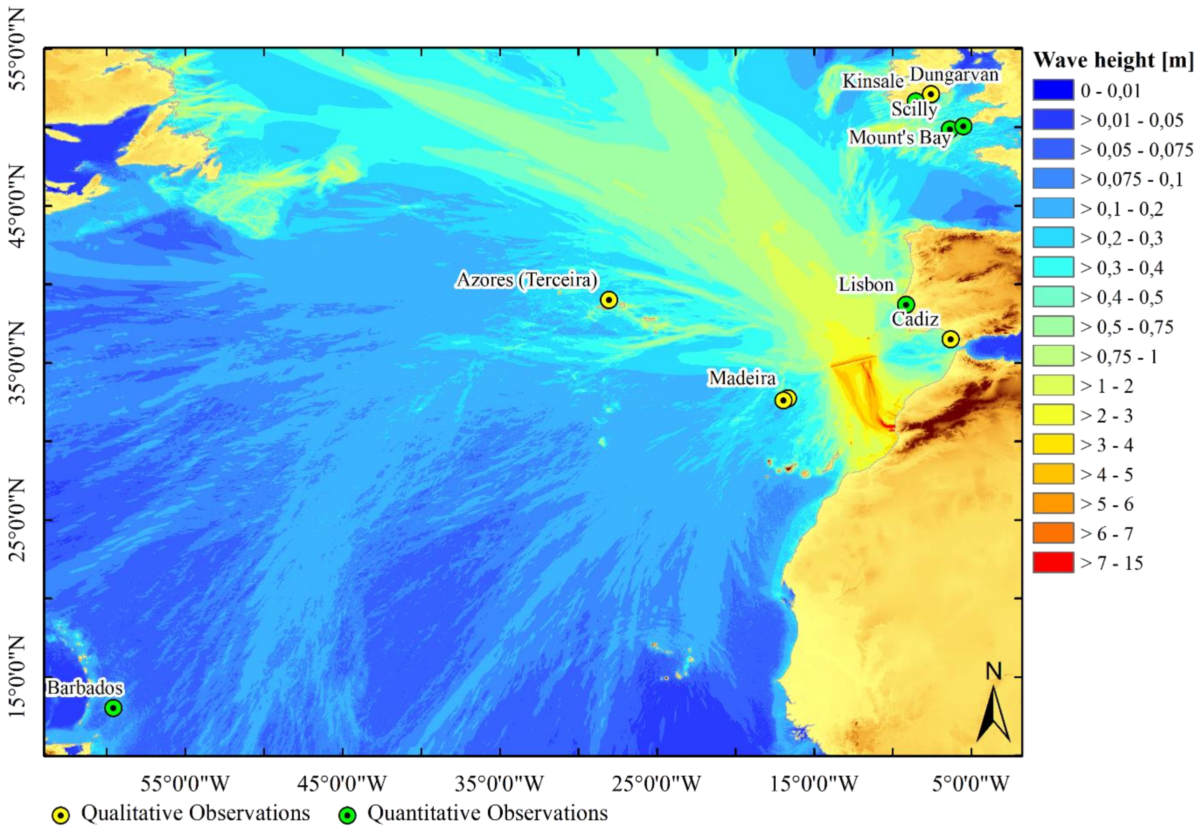

Figure 6. Maximum wave height distribution (color scale in m) in the Atlantic basin produced by the source of hypothesis B.

Figure 7 presents the corresponding synthetic tsunami waveforms at the VTGs. Table 4 gives a summary of the results. The analysis of the synthetic waveforms shows that a small withdraw of about 0.2 m arrives in Lisbon after 1 hour and 15 minutes followed by a water surface elevation of 0.9 m. The third wave has a maximum positive amplitude of 2.2 m (Fig. 7 (a)).

The maximum wave heights at the Scilly Islands is 0.5 m (Fig. 7 (b)). The first wave reaches 0.4 m, arriving close to 4 h after the earthquake. The synthetic tsunami waveform shows around 15-minute wave period. In Mount`s Bay, the first wave of 0.4 m arrives after 4 hours and 30 minutes with a 15-minute wave period (Fig. 7 (b)). Here, the maximum wave height, 0.7 m, comes more than 6 hours after the earthquake. In Kinsale, hypothesis B produces a maximum wave height of 0.6 m. The first wave of 0.2 m wave height in the VTG arrives after 4 hours and 15 minutes of tsunami propagation; here, the period is shorter than 15 min (Fig. 7 (c)).

In Madeira, the first and the maximum wave heights are greater in the eastern part of the island compared to the southern part. Maximum wave heights values reach 1.4 m in the east part of Madeira and 1.1 m in the south part of Madeira (Fig. 7 (d)). In the Azores, the wave height for Terceira island reaches up to 2.4 m (Fig. 7 (e)).

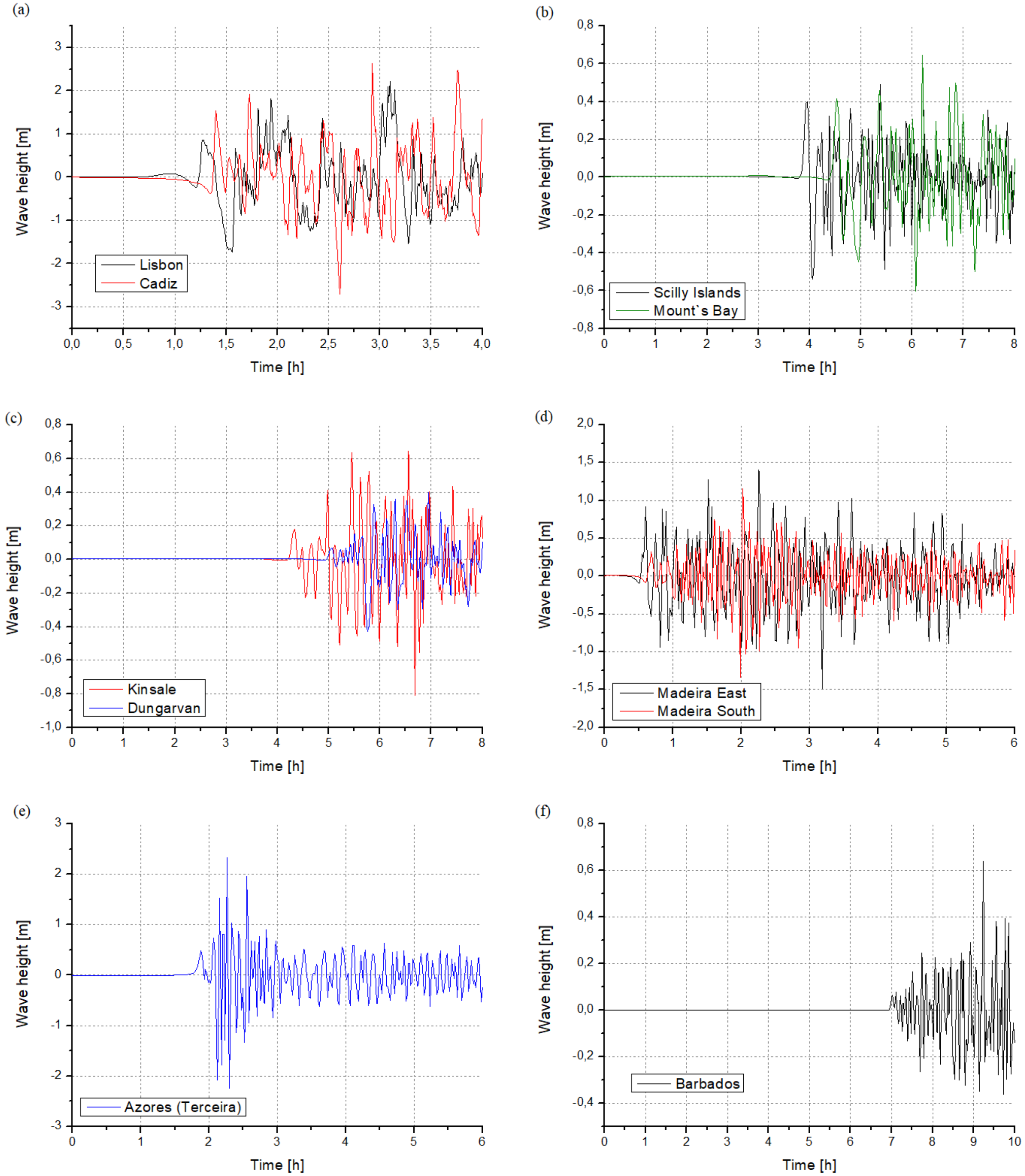

Figure 7. VTG records for hypothesis B at the coordinates of the locations presented in table 4.

Hypothesis B predicts a tsunami travel time of 7 hours to Barbados with the first peak of less than 0.1m and a maximum peak of 0.6 m after 9 hours and 15 minutes (Fig. 7 (f)). The first wave has a period slightly below 15 minutes. Table 4 gives a summary of the results for hypothesis B.

We also applied the Green's Law for this solution. The maximum wave height values after application of Green's Law are presented in table 4.

Table 4. Results of the VTGs for hypothesis B

Local		**VTG coordinates & depth**			**TTT**	**Wave height [m]**				**Polarity**	**Period**
		Lon. [°]	Lat. [°]	d [m]		First	max.	Green's Law	Obs.		
Lisbon		-9.136	38.706	3	~ 1 h 15 min	0.9 m	2.2 m	nesting	1.2 – 1.8 m	D	> 30 min
Cadiz		-6.291	36.524	4	~ 1 h	-0.4 m	2.6 m	nesting	-	D	~ 30 min
Scilly Islands		-06.383	49.85	50	< 4 h min	0.4 m	0.5 m	0.9 m	0.6 – 1.2 m	U	~ 15 min
Mount´s Bay		-05.48	50.08	26	~ 4 h 30 min	0.4 m	0.7 m	1 m	1.2 – 1.8 m	U	~ 15 min
Kinsale		-08.500	51.653	28	~ 4 h 15 min	0.2 m	0.6 m	1 m	0.6 m	U	< 15 min
Dungarvan		-07.479	51.949	50	~ 5 h	0.1 m	0.4 m	0.7 m	-	U	< 15 min
Madeira	**E**	-16.666	32.750	51	~ 30 min	0.9 m	1.4 m	2.5 m	-	U	~ 30 min
	S	-16.926	32.619	51	~ 40 min	0.3 m	1.1 m	2.1 m	-	U	~ 30 min
Azores		-27.150	38.800	53	~ 1 h 45 min	0.5 m	2.4 m	4.2 m	-	U	~ 15 min
Barbados		-59.566	13.033	50	~ 7 h	0.1 m	0.6 m	1.1 m	0.45 – 0.6 m	U	~ 30 min

6. Discussion and Conclusion

We investigated possible sources of the earthquake and tsunami on the 31st March 1761 earthquake in the Atlantic.

Firstly, we excluded the locations similar to the instrumental events of the 20th century: 25.11.1941 (Baptista et al., 2016) and 26.05.1975 (Kaabouben et al., 2009) because of incompatibility of tsunami travel times.

Secondly, we placed a source about 85 km to the east of the location proposed by Baptista et al. (2006) to include the Barbados travel time in our dataset (Fig. 2).

After setting the source position, we investigated focal mechanisms for the parent earthquake. We selected two focal mechanisms for testing: A and B. Solution A-MS corresponds to focal mechanism A with a multi-segment fault plane as described in section 4.2 (table 2).

Our tests produce a set of TTTs compatible with the observations with a 15-minute delay in the near-field and 30-minute delay in the far-field. These differences are acceptable considering that the location of the observation point is unknown. These results are valid for A, B and A-MS as the locations are similar. Tables 3 and 4 show that the predicted travel times are compatible with a source located in the area of the Coral Patch.

Any source located in the Northeast Atlantic south of the Scilly islands produces a shorter tsunami travel time to Scilly island than Mount's Bay. The 6 hours TTT reported in Kinsale contradicts the 4 hours TTT reported for Dungarvan (Fig. 1). On the other hand, the tsunami travel times predicted by our numerical simulation are consistent with their relative geographical position.

Source A produces wave heights applying the Green's Law to the values recorded at the VTGs which are compatible with the observations in Lisbon, Kinsale, Scilly and Barbados (Fig. 5 and table 3). The results of the synthetic wave records of Dungarvan, Madeira and the Azores are compatible with the observations. In Mount's Bay, the wave height computed using the Green's Law of the VTG value is smaller than the one reported. However, analysis of figure 4 shows that the computed maximum wave heights greater than 1.6 m for Mount's Bay. This value agrees with the observation.

Source B produces wave heights compatible with the observation in Lisbon, Scilly and Mount's Bay. We apply the Green's Law (Eq. 1) using the wave heights recorded at the VTG in Kinsale and Barbados and obtain larger wave heights than reported (table 4). Also, the modelled maximum wave heights in figure 6 are higher than 1.4 m, 2.2 m and 0.7 m for Kinsale, Scilly and Barbados respectively. These values are higher than the one observed. At the Azores, the wave height reaches 4.2 m (table 4); however, the descriptions do not report an inundation. Also, at the coast of Morocco, source B predicts wave heights close to 14 m. To our knowledge, the historical documents do not report any abnormal movement of the sea in Morocco.

The observations do not account for inundation in Lisbon. To investigate this fact, we estimated the tide condition in Lisbon for this day. To do this, we used a Moon Phase table (USNO, 2017) and concluded that the tide was 2.6 m above hydrographic zero (HZ) (in dropping tide conditions) at 1 p.m. on the 31st of March 1761 (table 5).

The maximum of the synthetic wave record for source A is 1.8 m about 2 hours and 15 minutes when the tide has dropped underneath 2.3 m above HZ. Adding 1.8 m to 2.3 m, we obtain 4.1m; this value is less than tide amplitude in spring tide condition. Considering that Lisbon downtown was rebuilt 3 m above sea level after the 1755 event (Baptista et al., 2011) the predicted wave heights are compatible with no flooding.

Source B produces a first wave of 0.9 but a maximum wave height of 2.2 m. The maximum wave height occurs at 15:00 o'clock and the estimated tide is approximately 2.1 m above HZ. Adding 2.2 to 2.1 we reach spring tide condition of 4.3 m.

Given the considerations above the tide, analysis favors solution A.

Table 5. Tide levels at the time of the earthquake and tsunami arrival.

	Time	**Tide condition**	**Estimated height relative to Hydrographic Zero**
Earthquake	Noon	Full tide	2.9 m
Tsunami arrival time	13:15	Dropping tide	2.6 m
Max. wave height Hyp. AMS	14:15	Dropping tide	2.3 m

Max. wave height Hyp. B	15:00	Dropping tide	2.1 m

The tidal range in Barbados is about 1 m. This small range might favor the observability of small first waves at tsunami arrival. For source A, the first wave in Barbados is about 0.1 m which raises the question if people might have noticed the advance of the sea. Close to 9 o'clock 2 hours after tsunami arrival, the peak at the VTG is higher than 0.2 m which results in 0.4 m when estimating the wave height applying the Green's Law for 5 m depth close to the shore. The coeval sources report similar wave height values.

Also, for source B, the wave height is smaller than 0.1 m at the VTG at the time of tsunami arrival. About 45 minutes later the waves are large than 0.2 m. The maximum peak occurs ca. 2 hours after tsunami arrival at 9 o'clock.

The small tide amplitude in Barbados does not contribute to select among the two candidate sources.

The summary (Annual register, 1761) states that the waves seemed to abate but at 10 o'clock started again with higher intensity and lasted until the next morning. This observation of greater amplitudes some hours after tsunami arrival fits for both sources. However, the timings of increasing wave heights do not match.

In Cadiz, both sources produce the observed withdrawal. In source A and B predict a drawdown of 0.6 m and 0.4 m respectively. High tide in Cadiz is about 1 hour earlier than in Lisbon. Once the tide was in dropping conditions at the time of the tsunami arrival a larger drawdown is more likely to be observed.

Considering the points discussed above, we conclude our preferred solution is A-MS. Following facts justify our choice:

• The candidate source in hypothesis A-MS is compatible with the geodynamic setting predicted by the NUVEL 1A model (DeMets et al., 1999). NE/SW compressive structures with similar fault plane parameters have been identified close to the Coral Patch seamount (Fig. 1) (Martinez-Loriente et al., 2013).

• The wave heights produced by the numerical models are in better agreement with hypothesis A-MS.

• Wave heights greater than 14 m produced by solution B would result in a catastrophic scenario which is rather unlikely and nor observed neither or reported. Also, 4.2 m wave height produced by hypothesis B in the Azores would have caused inundation, which has not been reported.

• Although both solutions follow our considerations for Lisbon, the wave heights generated by source A-MS seem more reasonable and close to the observed fluctuation of 2.4 m than the wave heights produced by source B.

• The larger drawdown in Cadiz favors solution A-MS.

• It is possible to find a geological source compatible with the source area deduced from TTTs and with macro-seismic intensity data (Baptista et al., 2006).

• The re-evaluated TTT for Barbados is consistent with the source location proposed here.

• The tectonic source proposed to reproduce the observations of the 31st March 1761 tsunami is located southwest of the source of the 1st November 1755 event in the SWIM.

This study together with the study by Baptista et al. (2006) underlines the need to include the 1761 event in all seismic and tsunami hazard assessments in the Northeast Atlantic basin.

Acknowledgements. This work is funded by FCT (Instituto Dom Luiz; FCT PhD grant ref. **PD/BD/135070/2017**). The authors wish to thank the editor Ira Didenkulova and the reviewers Uri S. ten Brink and Ceren Özer Sözdinler for their constructive comments and suggestions that greatly helped to improve this manuscript.

References

Annual Register: Volume 4, pages 92-95, 1761.

Argus, D. F., Gordon, R. G., DeMets, C., and Stein, S.: Closure of the Africa-Eurasia-North America plate motion circuit and tectonics of the Gloria fault. Journal of Geophysical Research: Solid Earth, 94(B5), 5585-5602, doi:10.1029/JB094iB05p05585, 1989.

Baptista, M. A., Miranda, P. M. A., Miranda, J. M., and Victor, L. M.: Constrains on the source of the 1755 Lisbon tsunami inferred from numerical modelling of historical data on the source of the 1755 Lisbon tsunami, Journal of Geodynamics, 25(1-2), 159-174, https://doi.org/10.1016/S0264-3707(97)00020-3, 1998a.

Baptista, M. A., Heitor, S., Miranda, J. M., Miranda, P., and Victor, L. M.: The 1755 Lisbon tsunami; evaluation of the tsunami parameters. Journal of Geodynamics, *25*(1-2), 143-157, 1998b.

Baptista, M. A., Miranda, J. M., Chierici, F., and Zitellini, N.: New study of the 1755 earthquake source based on multi-channel seismic survey data and tsunami modeling, Nat. Hazards Earth Syst. Sci., 3, 333-340, https://doi.org/10.5194/nhess-3-333-2003, 2003.

Baptista, M. A., Miranda, J. M., and Luis, J. F.: In search of the 31 March 1761 earthquake and tsunami source, Bulletin of the Seismological Society of America, 96(2), 713-7211, doi:10.1785/0120050111, 2006.

Baptista, M. A., Miranda, J. M., Lopes, F. C., and Luis, J. F.: The source of the 1722 Algarve earthquake: evidence from MCS and Tsunami data. Journal of Seismology, 11(4), 371-380, https://doi.org/10.1007/s10950-007-9058-y, 2007.

Baptista, M. A. and Miranda, J. M.: Revision of the Portuguese catalog of tsunamis, Nat. Hazards Earth Syst. Sci., 9, 25-42, https://doi.org/10.5194/nhess-9-25-2009, 2009.

Baptista, M. A., Miranda, J. M., Batlló, J., Lisboa, F., Luis, J., and Maciá, R.: New study on the 1941 Gloria Fault earthquake and tsunami, Nat. Hazards Earth Syst. Sci., 16, 1967-1977, https://doi.org/10.5194/nhess-16-1967-2016, 2016.

Baptista, M. A., Miranda, J. M., Matias, L., and Omira, R.: Synthetic Tsunami Waveform Catalogs With Kinematic Constraints, Nat. Hazards Earth Syst. Sci. Discuss., https://doi.org/10.5194/nhess-2017-57, 2017.

Barkan, R., Uri, S., and Lin, J.: Far field tsunami simulations of the 1755 Lisbon earthquake: Implications for tsunami hazard to the US East Coast and the Caribbean, Marine Geology, 264(1-2), 109-122, https://doi.org/10.1016/j.margeo.2008.10.010, 2009.

Bellin, J. N.: Carte hydrographique de La Baye De Cadix. 1762.

Blanc, P. L.: The tsunami in Cadiz on 1 November 1755: A critical analysis of reports by Antonio de Ulloa and by Louis Godin, Comptes Rendus Geoscience, 340(4), 251-261, https://doi.org/10.1016/j.crte.2007.12.001, 2008.

Blaser, L., Krüger, F., Ohrnberger, M., and Scherbaum, F.: Scaling relations of earthquake source parameter estimates with special focus on subduction environment, Bulletin of the Seismological Society of America, 100(6), 2914-2926, https://doi.org/10.1785/0120100111, 2010.

Borlase, W.: Some Account of the extraordinary Agitation of the Waters in Mount's-bay, and other Places, on the 31st of March 1761: In a Letter for the Reverend Dr. C Lyttelton, Philosophical Transactions of the Royal Society, vol. 52, Page 418-431, 1762.

Custódio, S., Dias, N. A., Carrilho, F., Góngora, E., Rio, I., Marreiros, C., Morais, I., Alves, P., and Matias, L.: Earthquakes in western Iberia: Improving the understanding of lithospheric deformation in a slowly deforming region, Geophysical Journal International, 203(1), 127-145, https://doi.org/10.1093/gji/ggv285, 2015.

DeMets, C., Gordon, R. G., Argus, D. F., and Stein, S.: Current plate motions. Geophysical journal international, 101(2), 425-478, 1990.

DeMets, C., Gordon, R. G., Argus, D. F., and Stein, S.: Effect of recent revisions to the geomagnetic reversal time scale on estimates of current plate motions, Geophysical research letters, 21(20), 2191-2194, doi:10.1029/94GL02118, 1994.

DeMets, C. and Dixon, T. H.: New kinematic models for Pacific-North America motion from 3 Ma to present, I: Evidence for steady motion and biases in the NUVEL-1A model. Geophysical Research Letters, 26(13), 1921-1924, doi:10.1029/1999GL900405, 1999.

Duarte, J. C., Rosas, F. M., Terrinha, P., Schellart, W. P., Boutelier, D., Gutscher, M. A., and Ribeiro, A.: Are subduction zones invading the Atlantic? Evidence from the southwest Iberia margin, Geology, 41(8), 839-842, https://doi.org/10.1130/G34100.1, 2013.

Fearns, J.: Letter to The London Chronicle N. 731, page. 214, 1761.

Fernandes, R. M. S., Bastos, L., Miranda, J. M., Lourenço, N., Ambrosius, B. A. C., Noomen, R., and Simons, W.: Defining the plate boundaries in the Azores region, Journal of Volcanology and Geothermal Research, 156(1), 1-9, https://doi.org/10.1016/j.jvolgeores.2006.03.019, 2006.

Fernandes, R. M. S., Miranda, J. M., Meijninger, B. M. L., Bos, M. S., Noomen, R., Bastos, L., Ambrosius, B. A. C., Riva, R. E. M.: Surface velocity field of the Ibero-Maghrebian segment of the Eurasia-Nubia plate boundary. *Geophysical Journal International*, *169*(1), 315-324, 2007.

GEBCO: http://www.gebco.net, The General Bathymetric Chart of the Oceans, GEBCO_2014 grid, version 20150318, 2014, last access: 1 February 2018.

Green, G.: On the motion of waves in a variable canal of small depth and width. Transactions of the Cambridge Philosophical Society, 6, 457, 1838.

Gutenberg, B. and Richter, C. F.: Seismicity of the Earth and associated phenomena, Princeton University Press, Princeton, New Jersey, 1949.

Gutscher, M. A., Malod, J., Rehault, J. P., Contrucci, I., Klingelhoefer, F., Mendes-Victor, L., and Spakman, W.: Evidence for active subduction beneath Gibraltar, Geology, 30(12), 1071-1074, https://doi.org/10.1130/0091-7613(2002)030<1071:EFASBG>2.0.CO;2, 2002.

Gutscher, M-A., Baptista, M, A, and Miranda, J. M.: The Gibraltar Arc seismogenic zone (part 2): constraints on a shallow east dipping fault plane source for the 1755 Lisbon earthquake provided by tsunami modeling and seismic intensity, Tectonophysics 426.1, 153-166, https://doi.org/10.1016/j.tecto.2006.02.025, 2006.

Gutscher, M. A., Dominguez, S., Westbrook, G. K., Le Roy, P., Rosas, F., Duarte, J. C., Terrinha, P., Miranda, J. M., Graindorge, D., Sallares, V., and Bartolome, R.: The Gibraltar subduction: A decade of new geophysical data. Tectonophysics, 574, 72-91, DOI 10.1016/j.tecto.2012.08.038, 2012.

Heberden, T.: An Account of the Earthquake felt in the Island of Madeira, March 31, 1761. Communicated by W Heberden, Philosophical Transactions of the Royal Society, vol. 52, pag. 155, 1761.

Instituto Geográfico Nacional: http://www.ign.es/web/ign/portal/sis-catalogo-terremotos/, last access: 1 February 2018.

Johnston, A. C.: Seismic moment assessment of earthquakes in stable continental regions—III, New Madrid 1811–1812, Charleston 1886 and Lisbon 1755, Geophysical Journal International, 126(2), 314-344, https://doi.org/10.1111/j.1365-246X.1996.tb05294.x, 1996.

Journal Historique: Suite de La Clef ou Journal Historique sur Les Matieres du Tems, contenant quelques nouvelles de Litterature, et autres Remarques curieuses, Juin 1773, Premiere Partie, Tome CXIII, Paris 462-464, 1773 (in French).

Kaabouben, F., Brahim, A. I., Toto, E., Baptista, M. A., Miranda, J. M., Soares, P., & Luis, J. F.: On the focal mechanism of the 26.05. 1975 North Atlantic event contribution from tsunami modeling. Journal of seismology, 12(4), 575-583, 2008.

Kaabouben, F., Baptista, M. A., Iben Brahim, A., El Mouraouah, A., and Toto, A.: On the moroccan tsunami catalogue, Nat. Hazards Earth Syst. Sci., 9, 1227-1236, https://doi.org/10.5194/nhess-9-1227-2009, 2009.

Laughton, A. S. and Whitmarsh, R. B.: The Azores-Gibraltar plate boundary, in: Geodynamics of Iceland and the North Atlantic area, NATO Advanced Study Institute, Reykjavik, Springer, the Netherlands, 63–81, https://doi.org/10.1007/978-94-010-2271-2_5, 1974.

Liu, P. L. F., Cho, Y. S., Briggs, M. J., Kanoglu, U., and Synolakis, C. E.: Runup of solitary waves on a circular island, Journal of Fluid Mechanics, 302, 259-285, https://doi.org/10.1017/S0022112095004095, 1995.

Liu, P. L., Woo, S. B., and Cho, Y. S.: Computer programs for tsunami propagation and inundation, Cornell University, available at: http://tsunamiportal.nacse.org/documentation/COMCOT_tech.pdf, last access: 1 February 2018, 1998.

Luis, J. F.: Mirone: A multi-purpose tool for exploring grid data, Computers & Geosciences, 33(1), 31-41, https://doi.org/10.1016/j.cageo.2006.05.005, 2007.

Lynnes, C. S. and Ruff, L. J.: Source process and tectonic implications of the great 1975 North Atlantic earthquake, Geophys. J. Int., 82, 497–510, 1985.

Manighetti, I., Campillo, M., Bouley, S., and Cotton, F.: Earthquake scaling, fault segmentation, and structural maturity. Earth and Planetary Science Letters, 253(3-4), 429-438, https://doi.org/10.1016/j.epsl.2006.11.004, 2007.

Mansinha, L. and Smylie, D. E.: The displacement fields of inclined faults, Bulletin of the Seismological Society of America, 61(5), 1433-1440. 1971.

Martínez-Loriente, S., Gràcia, E., Bartolome, R., Sallarès, V., Connors, C., Perea, H., Lo Iacono, C., Klaeschen, D., Terrinha P., Dañobeitia J. J., and Zitellini, N.: Active deformation in old oceanic lithosphere and significance for earthquake hazard: Seismic imaging of the Coral Patch Ridge area and neighboring abyssal plains (SW Iberian Margin), Geochemistry, Geophysics, Geosystems, 14(7), 2206-2231, doi:10.1002/ggge.20173, 2013.

Mason, A., Letter to the Reverend Thomas Birch, D. D. Secretary to the Royal Society, relating to an extraordinary agitation of the Sea there, 31st of March 1761, Philosophical Transactions of the Royal Society, vol. 52, page 477-478, 1761.

Mallet, Robert and John Wm. Mallet: The Earthquake Catalogue of the British Association, Transactions of the British Association for the Advancement of Science, 1852 to 1858, Reports 3 and 4, Taylor and Francis, London, 800 pp, 1858.

Mezcua, J., and Solares, J. M. M.: Sismicidad del área Ibero-mogrebí, I.G.N., nº 203, Madrid, 301 pp, http://www.ign.es/web/resources/sismologia/publicaciones//SismicidaddelAreaIberoMogrebi.pdf, 1983.

Miranda, J. M., Baptista, M. A., and Omira, R.: On the use of Green's summation for tsunami waveform estimation: a case study, Geophysical Journal International, 199(1), 459-464. https://doi.org/10.1093/gji/ggu266, 2014.

Molloy, M.: Philosophical Transactions of the Royal Society, Vol. 52, Page 142-143, 1761.

Moreira, V. S.: Sismicidade histórica de Portugal Continental, Rev. Inst. Nac. Met. e Geofísica, Março, 1984, 3–79, 1984.

National Geophysical Data Center / World Data Service (NGDC/WDS): Global Historical Tsunami Database. National Geophysical Data Center, NOAA, https://www.ngdc.noaa.gov/hazard/tsu_db.shtml, doi:10.7289/V5PN93H7, last access: 1 February 2018.

Nocquet, J. M., and Calais, E.: Geodetic measurements of crustal deformation in the Western Mediterranean and Europe. *Pure and applied geophysics*, *161*(3), 661-681, 2004.

Oliveira, C. S.: A sismicidade Histórica em Portugal Continental e a Revisão do Catálogo sísmico Nacional, Laboratório Nacional de Engenharia Civil, Proc. 36/1177638, 235, Lisboa, Portugal, 1986.

Omira, R., Baptista, M.A., and Matias, L.: Probabilistic tsunami hazard in the Northeast Atlantic from near-and far-field tectonic sources, Pure and Applied Geophysics 172 (3-4), 901-920, ISSN: 0033-4553 (Print) 1420-9136 (Online), https://doi.org/10.1007/s00024-014-0949-x, 2015.

Ribeiro, A., Mendes-Victor, L., Cabral, J. M. L. C., Matias, L., and Terrinha, P.: The 1755 Lisbon earthquake and the beginning of closure of the Atlantic, European Review, 14(2), 193-205, doi:10.1017/S1062798706000196, 2006.

Rocque, J.: A Plan of the City of Cadiz and the environs with the Harbour, Bay and Soundings at Low Water also a Particular Plan of the Town and Fortifications from the Collection of Capt. Clark and Improved by the late John Rocque, Topographer to his Majesty. Bibliothèque nationale de France, département Cartes et plans, CPL GE DD-2987, 1762.

Rosas, F. M., Duarte, J. C., Terrinha, P., Valadares, V., and Matias, L.: Morphotectonic characterization of major bathymetric lineaments in Gulf of Cadiz (Africa–Iberia plate boundary): insights from analogue modelling experiments, Marine Geology 261 (1-4), 33-47, https://doi.org/10.1016/j.margeo.2008.08.002, 2009.

Solares, J. M. and Lopez-Arroyo, A.: The great historical 1755 earthquake: Effects and damage in Spain, J. Seismol., 8, 275–294, https://doi.org/10.1023/B:JOSE.0000021365.94606.03, 2004.

Synolakis, C. E., Bernard, E. N., Titov, V. V., Kânoğlu, U., and Gonzalez, F. I.: Validation and verification of tsunami numerical models, In Tsunami Science Four Years after the 2004 Indian Ocean Tsunami 2197-2228, Birkhäuser Basel, doi:10.1007/s00024-004-0427-y, 2008.

Terrinha, P. , Matias, L., Vicente, J., Duarte, J., Luís, J., Pinheiro, L., Lourenço, N., Diez, S. Rosas, F., Magalhães, V., Valadares, V., Zitellini, N., Roque, C., Mendes Víctor, L. and MATESPRO Team.: Morphotectonics and strain partitioning at the Iberia–Africa plate boundary from multibeam and seismic reflection data, Marine Geology, 267, 3-4, 156-174, https://doi.org/10.1016/j.margeo.2009.09.012, 2009.

UC-IGN: Tsunami inundation maps along the south west Spanish coast, deliverable d7.1 of the 6th European framework programme project TRANSFER. http://www.transferproject.eu/, last access: 1. August 2018, 2009.

Unknown: An Account of the Earthquake at Lisbon, 31st March 1761: In a Letter from thence, dated 2nd April 1761, to Joseph Salvador, Esq. F.R.S. Philos. Trans. Letter XXVI. pp. 141-142, 1761.

United States Naval Observatory (USNO): http://aa.usno.navy.mil/data/docs/MoonPhase.php, last access: 1 February 2018, 2017.

Wells, D. L. and Coppersmith, K. J.: New empirical relationships among magnitude, rupture length, rupture width, rupture area, and surface displacement, Bulletin of the seismological Society of America, 84(4), 974-1002, 1994.

Wronna, M., Omira, R., and Baptista, M. A.: Deterministic approach for multiple-source tsunami hazard assessment for Sines, Portugal, Nat. Hazards Earth Syst. Sci., 15, 2557-2568, https://doi.org/10.5194/nhess-15-2557-2015, 2015.

Wronna, M., Baptista, M. A., and Götz, J.: On the construction and use of a Paleo-DEM to reproduce tsunami inundation in a historical urban environment–the case of the 1755 Lisbon tsunami in Cascais. Geomatics, Natural Hazards and Risk, 8(2), 841-862, https://doi.org/10.1080/19475705.2016.1271832, 2017.

Zitellini, N., Chierici, F., Sartori, R., and Torelli, L.: The tectonic source of the 1755 Lisbon earthquake and tsunami, Annals of Geophysics, 42(1), http://dx.doi.org/10.4401/ag-3699, 1999.

Zitellini, N., Mendes, L. A., Cordoba, D., Dañobeitia, J.J., Nicolich, R., Pellis, G., Ribeiro, A., Sartori, R., Torelli, L., Bartolome, R., Bortoluzzi, G., Calafato, A., Carrilho, F., Casoni, L., Chierici, F., Corela, C., Correggiari, A., Vedova, B. Della, Gracia, E., Jornet, P., Landuzzi, M., Ligi, M., Magagnoli, A., Marozzi, G., Matias, L., Penitenti, D., Rodriguez, P., Rovere, M., Terrinha, P., Vigliotti, L., and Ruiz, A. Zahinos:.Source of 1755 Lisbon earthquake and tsunami investigated. Eos, Transactions American Geophysical Union,82(26), 285-291, doi:10.1029/EO082i026p00285-01, 2001.

Zitellini, N., Gràcia, E., Matias, L., Terrinha, P., Abreu, M. A. DeAlteriis, G., Henriet, J.P., Dañobeitia, J.J., Masson, D.G., Mulder, T., Ramella, R., Somoza, L., and Diez, S.: The quest for the Africa–Eurasia plate boundary west of the Strait of Gibraltar, Earth and Planetary Science Letters, 280, 1-4, 13-50, https://doi.org/10.1016/j.epsl.2008.12.005, 2009.